ACS OMEGA

http://pubs.acs.org/journal/acsodf

Article

Metal-Decorated Phthalocyanine Monolayer as a Potential Gas Sensing Material for Phosgene: A First-Principles Study

Chen Wang, Yajun Wang, Qijun Guo, Enrui Dai, and Zhifeng Nie*

Cite This: *ACS Omega* 2022, 7, 21994−22002

Read Online

ACCESS | Metrics & More | Article Recommendations

ABSTRACT: Research into a gas sensing material with excellent performance to detect or remove toxic phosgene ($COCl_2$) is of great significance to environmental and biological protection. In the present work, the adsorption performance of $COCl_2$ on pristine phthalocyanine (Pc) and metal-decorated Pc (MePc, Me = Cu, Ga, and Ru) monolayers was studied by first-principles calculations. The results show that the absorption process of $COCl_2$ on pristine Pc and CuPc both belong to physisorption, indicating that they are not suitable gas sensing materials for $COCl_2$. When Pc sheets are decorated by Ga and Ru atoms, the adsorption of $COCl_2$ is changed into chemisorption, and the corresponding adsorption energies are −0.57 and −0.50 eV for GaPc and RuPc, respectively. The microcosmic mechanism between $COCl_2$ and adsorbents (GaPc, RuPc) was clarified by the analysis of the density of states, the charge density difference, and the Hirshfeld charge. In addition, the $COCl_2$ adsorption results in a significant conductivity variation of the RuPc monolayer, demonstrating it exhibits a high sensitivity to the $COCl_2$ molecule. Meanwhile, quick desorption processes were noticed at various temperatures for the $COCl_2$/RuPc system. Consequently, the RuPc monolayer can be considered as a potential candidate for phosgene sensors because of the moderate adsorption strength, high sensitivity, and fast desorption speed.

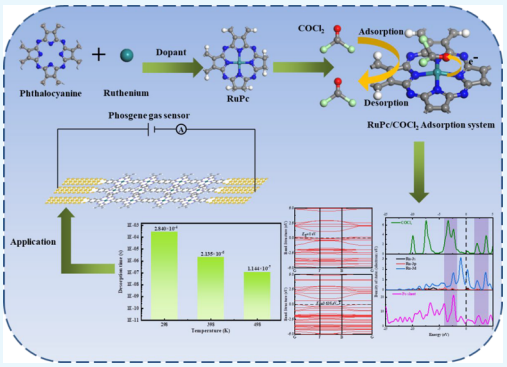

1. INTRODUCTION

Phosgene ($COCl_2$) is a colorless, highly toxic gas that has been used in chemical warfare as well as in industrial processes including the making of dyestuffs and polyurethane resins.[1] Once exposed to phosgene, the human respiratory system is severely damaged, leading to many diseases such as non-cardiogenic pulmonary edema, emphysema, and even death.[2,3] Because of the potential threat of phosgene, monitoring and controlling the concentration of phosgene in the environment is urgent. Currently, traditional metal oxide materials have been widely employed in detecting and capturing toxic gas.[4−7] However, the industrial applications of these materials are limited because of harsh working conditions, weak adsorption strength, poor sensitivity, and selectivity. To overcome these shortcomings, it is urgent to develop a kind of advanced gas sensing material with excellent performance for phosgene.

In recent years, massive researchers have conducted various investigations to improve the performance of gas sensing materials.,[8−12] Compared with the traditional sensing materials, two-dimension (2D) sensing materials have unique advantages in the design of new gas sensors because of the high surface area, excellent mechanical properties, suitable adsorption capacity, and numerous active sites.[13,14] Metal decorated phthalocyanine (MePc), which has a planar π aromatic structure, is a significant metal−organic molecular 2D material and exhibits a surprising variety of function.[15,16] Very recently, several metal-embedded phthalocyanine monolayers have been successfully synthesized in experiments, where these MePc exhibit high stability and good selectivity by decorating different metal atoms. For instance, Maggioni et al.[17] discovered that CuPc is a good gas sensor for oxynitride. Li et al.[18] studied the adsorption characteristics of H_2S on CuPc thin-film transistors by experiments and found that CuPc-based OTFT devices attached with a 195 nm insulator layer are potential gas sensors for hydrogen sulfide detection.

These aforementioned studies have confirmed the feasibility of metal phthalocyanines for the gas sensing, however, the microcosmic mechanism of gas-adsorbent interaction is difficult to be explained experimentally.[19,20] Thus, many researchers employed the density function theory (DFT) calculations to develop efficient and inexpensive gas sensing materials, and analyzed the microscopic interaction mechanism at the atomic or even electronic level. Generally, to detect and capture phosgene, two primary gas sensing materials have been

Received: April 24, 2022
Accepted: June 2, 2022
Published: June 13, 2022

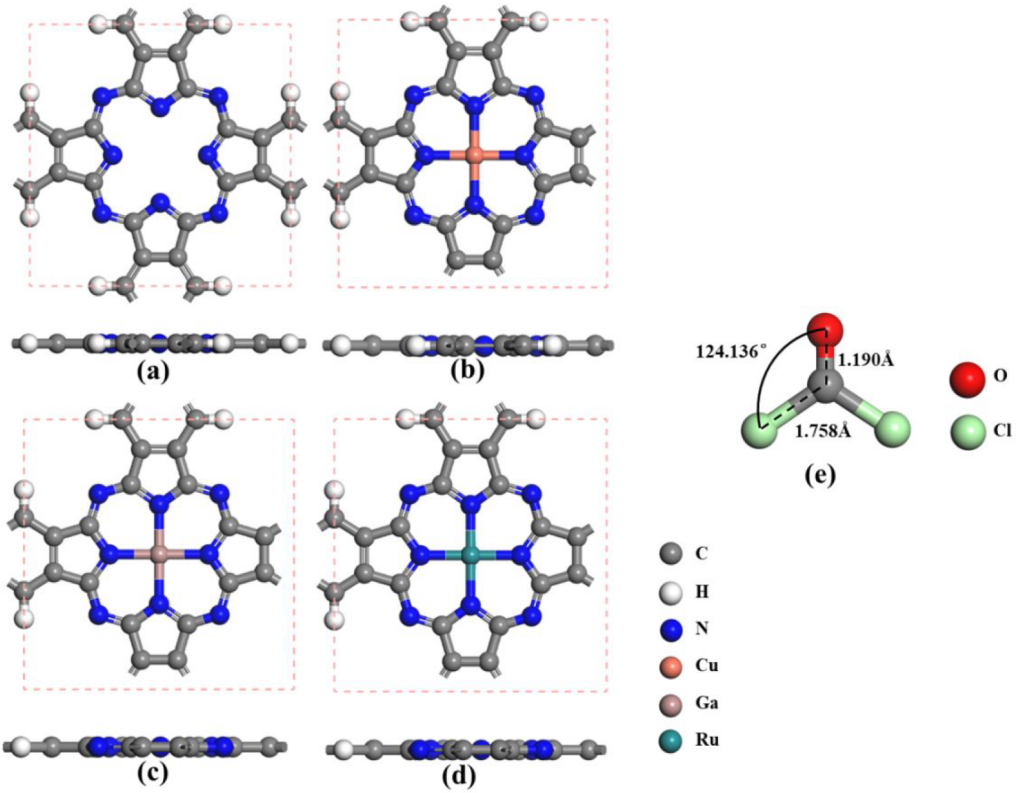

Figure 1. Geometric optimized model: (a) pristine Pc monolayer, (b) CuPc monolayer, (c) GaPc monolayer, (d) RuPc monolayer, and (e) gas molecule $COCl_2$. The C, H, N, Cu, Ga, Ru, O, and Cl atoms are indicated by gray, white, blue, orange, gray purple, blackish green, red, and green balls, respectively.

widely studied by the method of DFT: (1) the graphene family, such as metal-atom doped graphene,[21,22] white graphene,[23] and graphdiyne nanoflake;[24] and (2) 2D chalcogenides, such as MoS_2.[25] However, the microcosmic mechanism of phosgene gas adsorbed on metal-decorated phthalocyanine is lacking investigation. In this regard, we use the DFT method to simulate the adsorption behaviors of phosgene on phthalocyanine with and without metal atoms (Cu, Ga, and Ru) doping. The adsorption energy, density of states (DOS), total charge density (TCD), charge difference density (CDD), and band structure are systematically investigated. Meanwhile, the sensing mechanism based on the conductivity change and desorption time is also evaluated, which provides theoretical support to explore the MePc monolayer as a potential phosgene gas sensor/adsorbent.

2. COMPUTATIONAL METHODOLOGY

The density functional theory (DFT) calculations have been completed by the *Dmol*^{3} package in *Materials Studio* in this study.[26] The Perdew−Burke−Ernzerhof (PBE) of generalized gradient approximation (GGA) was used to treat the exchange-correlation effect of electrons.[27,28] The weak long-range interaction was corrected by adopting the empirical dispersion correction of Grimme (DFT-D).[29−31] The double numerical with polarization (DNP) basis and DFT semicore pseudopotential (DSSP) method was employed in the simulation process.[32,33] Moreover, the k points sampled by the Monkhorst−Pack scheme in the geometry optimization (electronic properties) calculations were set to 6 × 6 × 1 (12 × 12 × 1) and the global cutoff radius was selected as 5.2 Å.[34] Considering the effect of periodic image interaction, the vacuum layer along the Z direction was set to 20 Å.[35] In geometric optimization, energy tolerance accuracy, maximum force tolerance, and maximum displacement were selected as 1.0×10^{-5} Ha, 0.002 Ha/Å, and 0.005 Å, respectively.[36]

The binding energy (E_{bin}) for metal decorated phthalocyanine monolayer is defined as

$$E_{bin} = E_{Me+Pc} - E_{Pc} - E_{Me} \quad (1)$$

Where $E_{Pc,}$ and E_{Me+Pc} represent the total energies of pristine and metal-doped Pc, respectively. E_{Me} is the energy of the corresponding volume of an isolated metal atom ($E_{Me(bulk)}$). In addition, the aggregation possibility of metal atoms in the phthalocyanine monolayer was explored by calculating the cohesive energy (E_{coh}). $E_{coh} = (E_{Me(bulk)} - E_{iso\text{-}Me})/n$, where $E_{iso\text{-}M}$ is the energy of a single metal atom and n is the volume number of metal atoms.

To assess the sensing ability, the adsorption energy (E_{ads}) of phosgene molecule on the pristine Pc and MePc monolayers are defined as

$$E_{ads} = E_{gas+MePc} - E_{MePc} - E_{gas} \quad (2)$$

Where $E_{gas+MePc}$ is the total energy of phosgene adsorbed on metal doped phthalocyanine, E_{MePc} and E_{gas} are the total energies of MePc monolayer and phosgene molecule, respectively.

In general, when E_{ads} is negative, the adsorption should be spontaneous, and a more negative value means a better stability.[36,37] If the absolute value of negative adsorption energy E_{ads} > 0.5 eV, the adsorption process can be judged as chemical adsorption, otherwise, it is physical adsorption.[10,38] In this work, the adsorption behavior of phosgene molecules on

https://doi.org/10.1021/acsomega.2c02548
ACS Omega 2022, 7, 21994−22002

phthalocyanine and metal phthalocyanine monolayers are calculated at room temperature (298 K). To reveal the interaction between substrate and gas molecules, Hirshfeld charge is calculated to discuss the corresponding charge transfer (Q_t) according to the following equation:

$$Q_t = Q_{\text{adsorbed molecule}} - Q_{\text{isolated molecule}} \quad (3)$$

$Q_{\text{adsorbed molecule}}$ and $Q_{\text{isolated molecule}}$ represent the charge numbers of target molecules before and after adsorption, respectively. When the charge transfer $Q_t > 0$, it indicates that the electrons are transferred from gas molecule to phthalocyanine surface, otherwise, the electrons are transferred from phthalocyanine surface to gas molecule.

3. RESULTS AND DISCUSSION

3.1. Structure and Stability of Pristine Pc, MePc, and $COCl_2$. Figure 1 shows the optimized geometries of pristine Pc, metal doped phthalocyanine (MePc, Me= Cu, Ga, and Ru) monolayers and gas molecule $COCl_2$. As shown in Figure 1a, the full-relaxed pristine Pc monolayer contains 20 C atoms, 8 N atoms, and 4 H atoms. All the atoms in each molecule are coplanar, indicating the whole molecule is fully delocalized and conjugated. When the Pc monolayer is decorated with Cu, Ga, and Ru atoms (Figure 1b–d), the CuPc, GaPc, and RuPc monolayer remain in the stable "graphene-like" plane configuration. The lattice constants of both phthalocyanine and metal phthalocyanine are about 10.69 Å, which is in good agreement with the published experimental and theoretical results.[39−41] Figure 1e gives the optimized geometrical structure of $COCl_2$ gas molecule. The bond lengths of C−O bond and C−Cl bond in the $COCl_2$ molecule are 1.190 and 1.758 Å, respectively, and their bond angles are 124.136°, which matches well with the other calculated results.[42]

The binding energy (E_{bin}) between the central metal and Pc monolayer is plotted in Figure 2, one can see that the E_{bin} of MePc (Me= Cu, Ga, and Ru) monolayer are −7.63 to −10.11 eV, and all of the values are below the cohesive energy of corresponding metal bulk, demonstrating they are stable. According to previous study, the center site, namely, the vacancy in the center of Pc or just above the doped metal atom in MePc, is selected as the preferential adsorption site.[43]

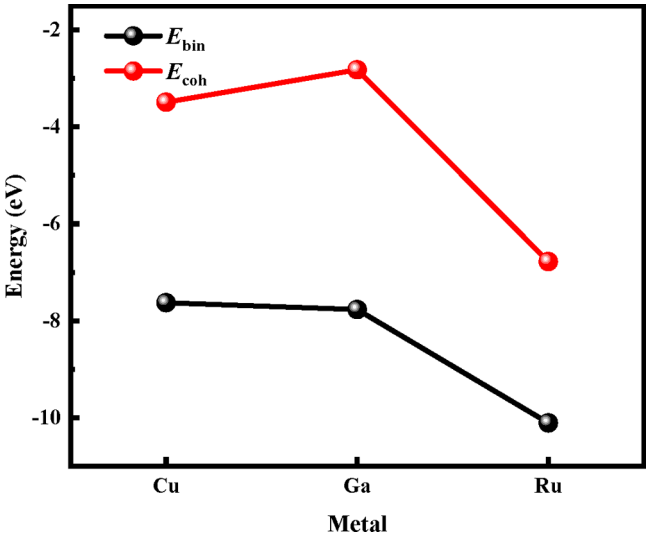

Figure 2. Cohesive energy of metal bulk (E_{coh}) and binding energy between central metal and Pc monolayer (E_{bin}) as a function of the different decorated metals.

3.2. Adsorption Behavior of $COCl_2$ on Pristine Pc and MePc. The best adsorption structure of $COCl_2$ on the pristine Pc and MePc (Me= Cu, Ga, and Ru) monolayer is described in Figure 3. The adsorption energy, charge transfer, and band gap of the pristine Pc system are listed in Table 1. In the present work, we consider the parallel and vertical adsorption style, for instance, the structure of $COCl_2$ parallelly adsorbed on the pristine Pc is defined as Pc-$COCl_2$-P, as seen in Figure 3a. After adsorption, the $COCl_2$ gas molecule is preferential to adsorb on the Pc substrate in parallel style, and the adsorption energy is −0.37 eV, with a charge of 0.0327 e transferred from the Pc substrate to $COCl_2$. The interaction between the $COCl_2$ molecule and Pc substrate can be regarded as physical adsorption, thus, the pristine Pc monolayer has poor $COCl_2$ capture ability.[33] The calculated adsorption parameters of $COCl_2$ on the MePc (Me = Cu, Ga, and Ru) monolayer substrate are summarized in Table 2. The $COCl_2$-P on the GaPc surface is thermodynamically unstable because it is changed into the adsorption style of $COCl_2$-V on the GaPc monolayer after relaxation. From Table 2, one can see that the $COCl_2$ molecule tends to be adsorbed on MePc sheets in parallel style except for the GaPc monolayer. The introduction of Ga and Ru atoms can obviously improve the adsorption ability of Pc toward $COCl_2$, the most stable adsorption structures are GaPc-$COCl_2$-V and RuPc-$COCl_2$-P with the E_{ads} of −0.57 eV and −0.50 eV, respectively, which are concluded as chemisorption.[33] However, the decoration of Cu atom cannot promote the $COCl_2$ capture ability because of the weak adsorption energy. From Figure 3c, d, the $COCl_2$ adsorbed on GaPc and RuPc substrates exhibit little deformation, and the corresponding adsorption distance (charge transfer) is 2.143 Å (0.1236 e) and 2.100 Å (0.1654 e), respectively. Those results indicate that the Ga and Ru atom doped Pc has stronger adsorption performance to $COCl_2$ in comparison with the pristine Pc.

The DOS of the lowest-energy configuration of $COCl_2$ on the pristine Pc is shown in Figure 4. One can see that the DOS of $COCl_2$ is nonlocalized, and there is no obvious resonance peak between the $COCl_2$ and Pc monolayer. This illustrates that the interaction between $COCl_2$ and the pure Pc monolayer is weak, which mainly relies on the van der Waals force. Thus, the pristine Pc monolayer could not be a good gas sensing material for $COCl_2$ because of its poor adsorption capacity.

Figure 5 shows the strong resonance peak (the light blue region) between the $COCl_2$ molecule, the decorated Ga atom, and the Pc sheet, which implies a significant interaction in $COCl_2$/GaPc adsorption system. By contrast, in the pristine Pc system (Figure 4), there only exists a weak interaction between $COCl_2$ and pure Pc sheet. Therefore, the doped Ga atom behaves as an electron bridge enhancing the interactions of gas-adsorbent. Additionally, there also exists the orbital hybridization between the $COCl_2$ and Pc sheet, as indicated by the orange dashed line. The strong interactions can be further confirmed by the charge density difference (CDD) and total charge density (TCD) corresponding to the $COCl_2$/GaPc adsorption system, as shown in Figure 6. The electron aggregation is mainly localized on the $COCl_2$ molecule, which manifests the electron-withdrawing property of $COCl_2$, this coincides with the Hirshfeld analysis (Q_t = −0.1236 e). The localized electron depletion is around the Ga atom, which also

https://doi.org/10.1021/acsomega.2c02548
ACS Omega 2022, 7, 21994−22002

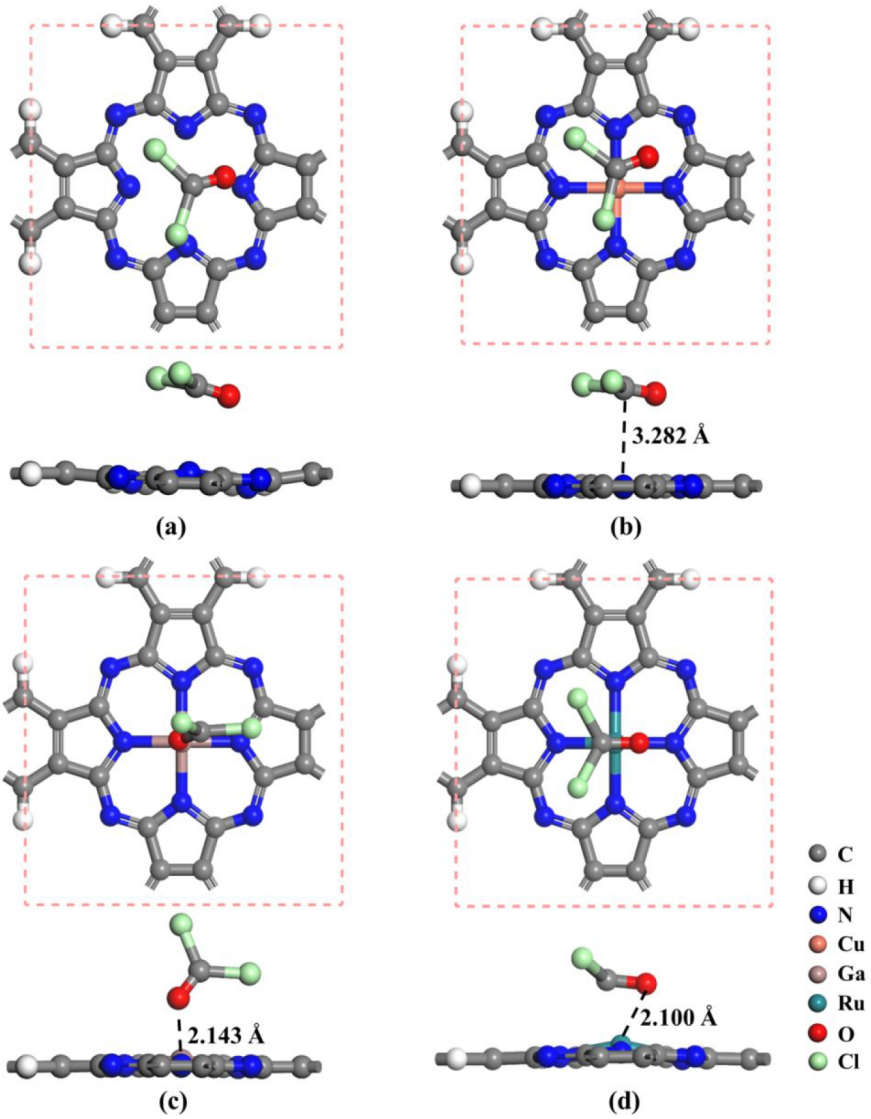

Figure 3. Top and side views of the geometric optimized structure after adsorption: (a) Pc-$COCl_2$-P, (b) CuPc-$COCl_2$-P, (c) GaPc-$COCl_2$-V, and (d) RuPc-$COCl_2$-P. The C, H, N, Cu, Ga, Ru, O, and Cl atoms are indicated by gray, white, blue, orange, gray purple, blackish green, red, and green balls, respectively.

Table 1. Adsorption Energy (E_{ads}) of Gas Molecule $COCl_2$ on the Pc Substrate, Charge Transfer between $COCl_2$ and Pc (Q_t, Negative Value Indicates That the Gas Has Gained Electrons), and Energy Gap (E_g) for Pc Adsorption System

gas	materials	adsorption style	E_{ads} (eV)	Q_t (e)	E_g (eV)
$COCl_2$	Pc	parallel	−0.37	0.0327	0.00
		vertical	−0.16	0.0046	0.00

Table 2. Adsorption Energy (E_{ads}) of Gas Molecule $COCl_2$ on CuPc, GaPc, and RuPc, Adsorption Distance (d), and Charge Transfer (Q_t) for Different Adsorption Systems

gas	materials	adsorption style	E_{ads} (eV)	d (Å)	Q_t (e)
$COCl_2$	CuPc	parallel	−0.30	3.282	−0.0504
		vertical	−0.15	2.881	−0.0369
	GaPc	vertical	−0.57	2.143	−0.1236
	RuPc	parallel	−0.50	2.100	0.1654
		vertical	−0.32	2.047	−0.1664

demonstrates that it denotes partial electrons (0.0589 e) to the $COCl_2$ molecule. Meanwhile, the $COCl_2$ molecule also takes 0.0647 e from the Pc sheet. In other words, Ga bridges the charge transfer from the gas molecule to the Pc monolayer, thus facilitating electron redistribution in the adsorbed system. Besides, the TCD predicts the overlap of electron density of $COCl_2$ gas molecules with the GaPc monolayer, as seen in Figure 6c, d. Consequently, the GaPc monolayer can be considered as candidate for phosgene adsorbent or gas sensor because of its strong removal ability.

To clarify the interaction mechanisms of the $COCl_2$/RuPc adsorption system, the DOS of $COCl_2$ adsorbed on RuPc monolayer is also calculated, as seen in Figure 7, indicating the strong resonance peak (the violet region) between the $COCl_2$ molecule, the Ru-3d orbitals, and the Pc sheet, which manifests a significant interaction in $COCl_2$/RuPc adsorption system. Thus, the decorated Ru atom acts as an electron bridge, strengthening the interactions between the adsorbed $COCl_2$ molecule and the Pc monolayer. The strong interactions are further confirmed by the CDD diagram in panels a and b in

https://doi.org/10.1021/acsomega.2c02548
ACS Omega 2022, 7, 21994−22002

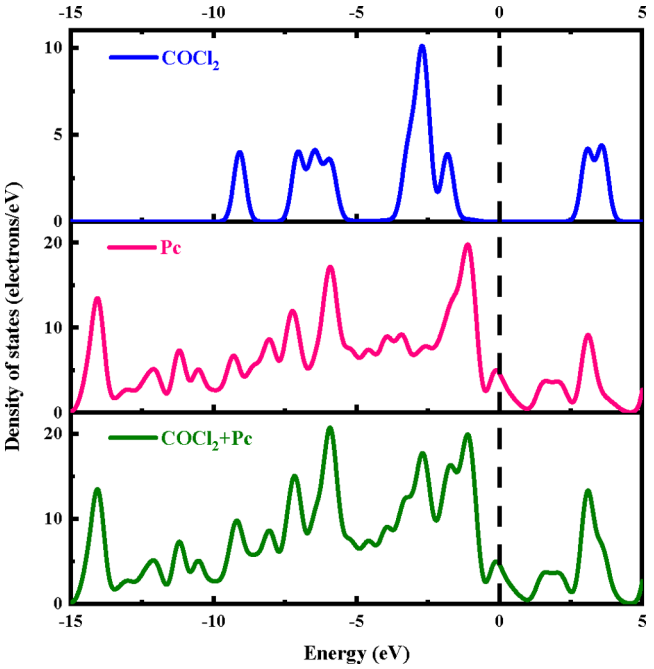

Figure 4. DOS of $COCl_2$, a Pc monolayer, and $COCl_2$ adsorbed on a Pc monolayer. The Fermi level is set to zero energy and indicated by the black dashed line.

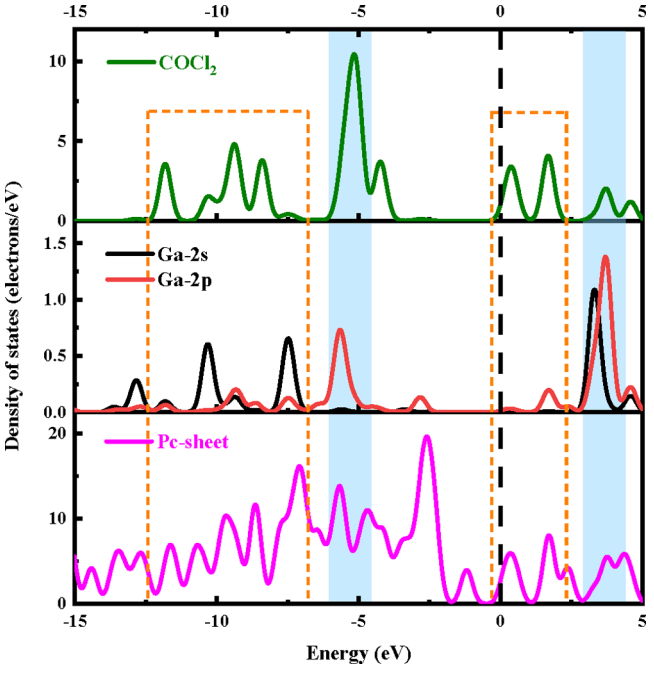

Figure 5. DOS of $COCl_2$ adsorbed on the GaPc monolayer. The Fermi level is set to zero energy and indicated by the black dashed line.

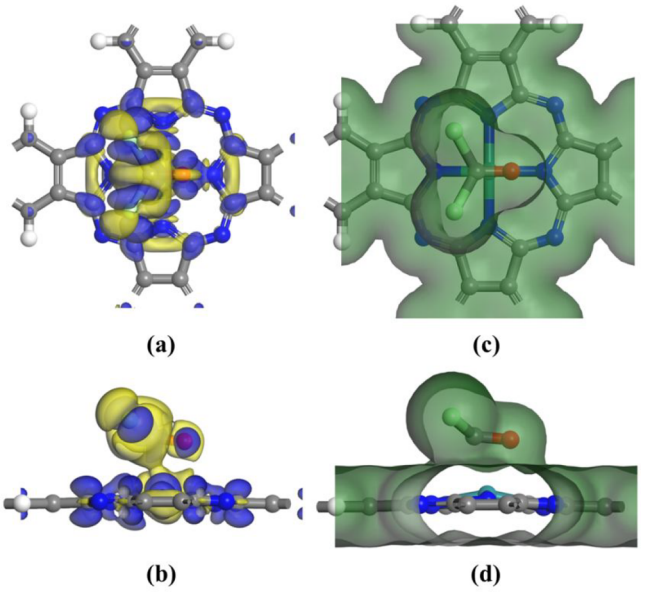

Figure 6. (a) Top and (b) side views of the charge density difference (CDD) map and (c) top and (d) side views of total charge density (TCD) map correspond to the most stable adsorption system of $COCl_2$ on GaPc. The blue (yellow) areas are electron aggregation (depletion), and the isosurface values of CDD and TCD are ±0.02 and ±0.05 e/Å^3, respectively.

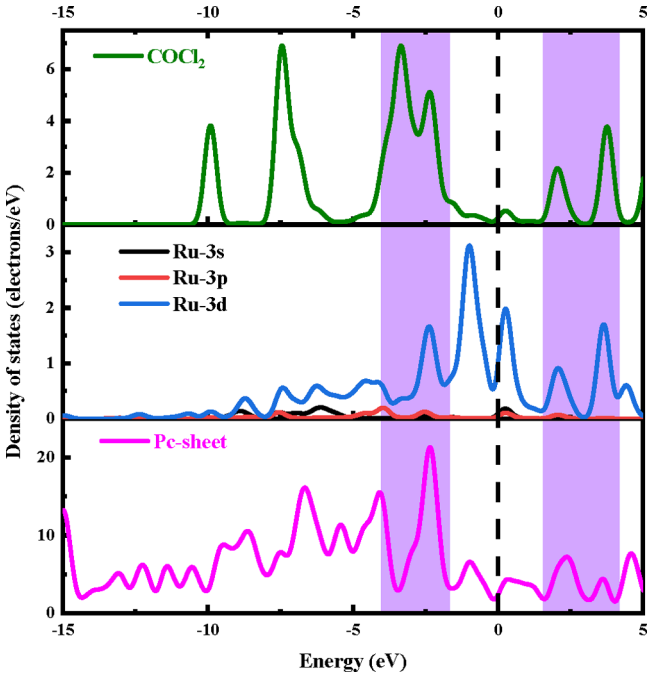

Figure 7. DOS of $COCl_2$ adsorbed on a RuPc monolayer. The Fermi level is set to zero energy and indicated by the black dashed line.

Figure 8, the dense electron aggregation is located between the Ru and O atoms, indicating its strong covalent bond. Unlike the adsorption system of $COCl_2$/GaPc (Figure 6), many electrons are accumulated around the doped Ru atom, and the Ru gains 0.1108 e from the gas molecule, which is consistent with the Hirshfeld analysis (Q_t = −0.1654 e), and thus the $COCl_2$ acts as an electron donor. The total electronic charge densities (TCD) of gas molecules absorbed on the RuPc monolayer in Figure 8c, d predict that there is an obvious electron orbital overlap between the gas molecules and the RuPc monolayer. Thus, the RuPc monolayer can be also considered as another candidate for phosgene adsorbent or gas sensor.

3.3. Analysis of the Sensing Mechanism. The above sections exhibit the characteristics of good stability and strong adsorption capacity of GaPc and RuPc monolayers, which is suitable for the potential $COCl_2$ gas sensing material. In this section, to better understand the microscopic sensing

https://doi.org/10.1021/acsomega.2c02548
ACS Omega 2022, 7, 21994−22002

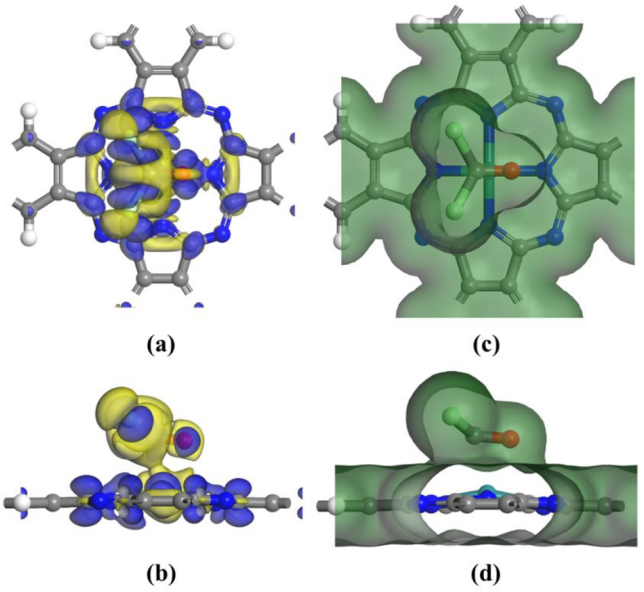

Figure 8. (a) Top and (b) side views of the charge density difference (CDD) map and (c) top and (d) side views of total charge density (TCD) map correspond to the most stable adsorption system of $COCl_2$ on RuPc. The blue (yellow) areas are electron aggregation (depletion), and the isosurface values of CDD and TCD are ±0.02 and ±0.05 e/Å^3, respectively.

mechanism, we further analyzed the sensitivity and desorption time for the GaPc and RuPc monolayers. Generally, the energy gap is used as an evaluation criterion to evaluate the exciting behavior of the molecule; a small energy gap usually fits a molecule that is easy to excite, and the results also reflect the change in conductivity of the system. Figure 9 shows the diagram of the energy gap of a Ga and Ru atom doped phthalocyanine before and after the $COCl_2$ gas molecule was adsorbed. According to Figure 9a, the Ga-doped Pc monolayer shows a semimetallic feature, with the electronic energy gap of the GaPc monolayer remains the same after the $COCl_2$ adsorption, as shown in Figure 9b. Thus, the conductive behavior between gas molecules and GaPc monolayer has little variation, demonstrating that it has poor $COCl_2$ sensibility. From panels c and d in Figure 9, the energy gap of the RuPc monolayer enlarged from 0 to 0.605 eV after the $COCl_2$ gas molecule adsorption, which indicated that the adsorption system changes from a semimetallic feature to a semiconductor. Because of the noticeable increase in the energy gap, the RuPc monolayers show excellent sensitivity. Consequently, compared with the GaPc monolayer, the RuPc monolayer is more suitable as a promising $COCl_2$ sensing material in the case of sensitivity.

It is well-known that the sensitivity can be assessed by exploring the variation of electrical conductivity (σ) of the $COCl_2$/MePc gas adsorption system, the variation in electrical conductivity could be defined as[23]

$$\sigma \propto \exp\left(\frac{-E_g}{2K_BT}\right) \tag{4}$$

where E_g is the band gap, K_B represents the Boltzmann constant (8.62×10^{-5} eV/K), and T is the working temperature of the gas sensor. According to the discussion above, the band gap of $COCl_2$/GaPc adsorption systems remains unchanged, which implies that there are few effects on the resistivity when the phosgene adsorbed on GaPc monolayer, thus the sensitivity of GaPc monolayer to phosgene molecules is poor. Meanwhile, upon exposure to the phosgene molecule, the electronic properties of the RuPc monolayer are dramatically changed, and there is an effectively interact between RuPc and $COCl_2$ according to the previous analysis.

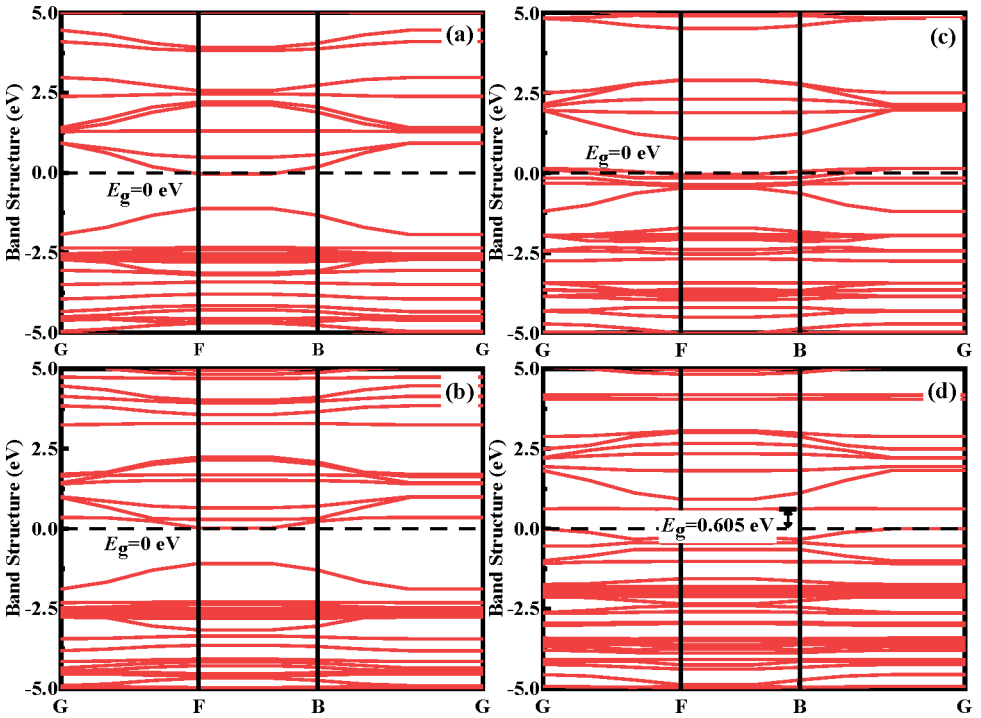

Figure 9. Band gap of GaPc (a) before $COCl_2$ adsorption and (b) after $COCl_2$ adsorption. The band gap of RuPc (c) before $COCl_2$ adsorption and (d) after $COCl_2$ adsorption. The dashed line is the Fermi energy.

https://doi.org/10.1021/acsomega.2c02548
ACS Omega 2022, 7, 21994−22002

This illustrates that doping phthalocyanine monolayer with Ru reflects the excellent applicability as a gas sensor for the detection of $COCl_2$.

Finally, the desorption property is also significant to assess the repeatability of a gas sensor. Moderate interactions between sheet and gas molecules imply that adsorbate can be desorbed in a short time so that the device can realize its sustainable utilization. On the basis of the transition state theory, we calculated desorption time (τ) by the following equation:[44]

$$\tau = \upsilon_0^{-1} \exp\left(\frac{-E_{ads}}{K_B T}\right) \quad (5)$$

where υ_0 is the attempt frequency, and T is the temperature. In this work, the value of attempt frequency is considered as 1×10^{-12} s^{-1}, which was employed by the reported literature.[25,45] The desorption time for the phosgene over RuPc at various temperatures is shown in Figure 10, where the working

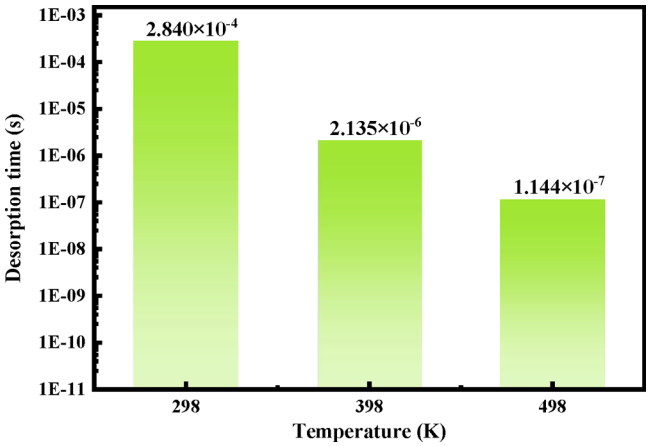

Figure 10. Desorption time for the phosgene over RuPc at various temperatures.

temperature is from 298 to 498 K. The results indicate that the desorption time of phosgene over RuPc monolayer decreases gradually (1.144×10^{-7} to 2.841×10^{-4} s) with the increase in temperature. Therefore, the sensitivity of RuPc to phosgene is large enough, and RuPc can be used as the sensor for gas detection because of the quick desorption time.

A comparative analysis of different 2D materials toward $COCl_2$ sensing with previously reported research work has been conducted, as shown in Table 3. First, it can be seen that the adsorption of phosgene on boromerene is physical adsorption, and the interaction is weak, so it is not suitable to be a gas sensing material for $COCl_2$.[45] We can see that Si embedded MoS_2 sheet and AlPc monolayer have strong adsorption capacity for phosgene molecules, which severely impedes gas desorption because of their long desorption time.[25,36] Therefore, they are not suitable for reusable $COCl_2$ gas sensor materials. In contrast, the RuPc monolayer can be considered as a potential and promising candidate for the $COCl_2$ gas sensor because of its moderate adsorption capacity and fast desorption speed.

Table 3. Comparison of Different Properties for $COCl_2$ Adsorbed on Different 2D Materials[a]

2D materials	E_{ads} (eV)	τ (s)	refs
Si-embedded MoS_2 sheet	−1.23	5.77×10^{8}	25
AlPc monolayer	−0.86	3.47×10^{2}	36
borophene	−0.31	1.74×10^{-7}	45
RuPc monolayer	−0.50	2.84×10^{-4}	this work

[a]The desorption time τ (at 298 K) is calculated from the data in the literature.

4. CONCLUSIONS

In this work, the first-principles calculation was employed to study the adsorption performance of $COCl_2$ on the pristine Pc and MePc (Me = Cu, Ga, and Ru), aiming to seek a novel MePc-based gas sensing material for detecting or removing phosgene. The results show that the pristine Pc and CuPc have less potential to be used as a gas sensing material for $COCl_2$ because of their poor adsorption strength; However, when decorating Ga and Ru atom into a Pc sheet, the decorated Ga, Ru atom acts as an electron bridge, enhancing the interactions between the adsorbed $COCl_2$ molecule and Pc monolayer. On the basis of the analysis of the energy gap, the RuPc monolayer exhibits a high sensitivity to the $COCl_2$ molecule because of the variation of conductivity. In addition, a quick response on the desorption was noticed for the $COCl_2$/RuPc substrate at various temperatures. Overall, the RuPc monolayer is one of the potential candidates for phosgene sensors, because it shows good stability, moderate adsorption strength, high sensitivity, and fast desorption speed.

AUTHOR INFORMATION

Corresponding Author

Zhifeng Nie − *Yunnan Key Laboratory of Metal−Organic Molecular Materials and Device, Kunming University, Kunming 650214, China;* orcid.org/0000-0002-4342-9902; Email: niezf123@163.com

Authors

Chen Wang − *Yunnan Key Laboratory of Metal−Organic Molecular Materials and Device, Kunming University, Kunming 650214, China; School of Physical Science and Technology, Kunming University, Kunming 650214, China*

Yajun Wang − *Yunnan Key Laboratory of Metal−Organic Molecular Materials and Device, Kunming University, Kunming 650214, China; School of Physical Science and Technology, Kunming University, Kunming 650214, China*

Qijun Guo − *Yunnan Key Laboratory of Metal−Organic Molecular Materials and Device, Kunming University, Kunming 650214, China; School of Chemistry and Chemical Engineering, Kunming University, Kunming 650214, China;* orcid.org/0000-0003-3915-6195

Enrui Dai − *School of Chemistry and Chemical Engineering, Kunming University, Kunming 650214, China*

Complete contact information is available at: https://pubs.acs.org/10.1021/acsomega.2c02548

Notes

The authors declare no competing financial interest.

ACKNOWLEDGMENTS

The authors gratefully acknowledge financial supports from National Natural Science Foundation of China (Grant 51904137), Special Basic Cooperative Research Programs of Yunnan Provincial Undergraduate Universities' Association

https://doi.org/10.1021/acsomega.2c02548
ACS Omega 2022, 7, 21994−22002

(Grant 202101BA070001-032), Basic Research Project of Yunnan Province (202201AT070017), and Scientific Research Funds of Yunnan Education Department (2022Y726, 2022Y718, 2022Y750). The authors also thank the High-Level Talent Plans for Young Top-notch Talents of Yunnan Province (Grant YNWR-QNBJ-2020-017) and High-Level Talent Special Support Plans for Young Talents of Kunming City (Grant C201905002).

REFERENCES

(1) Ghambarian, M.; Azizi, Z.; Ghashghaee, M. Remarkable improvement in phosgene detection with a defect-engineered phosphorene sensor: first-principles calculations. *Phys. Chem. Chem. Phys.* **2020**, *22*, 9677−9684.
(2) Qu, Y.; Zhang, L.; He, D.; Xu, N.; Tang, Y.; Shao, Y.; Shen, J. Protective role of mesenchymal stem cells transfected with miRNA-378a-5p in phosgene inhalation lung injury. *Biochem. Biophys. Res. Commun.* **2020**, *530*, 189−195.
(3) Liu, P.; Liu, N.; Liu, C.; Jia, Y.; Huang, L.; Zhou, G.; Li, C.; Wang, S. A colorimetric and ratiometric fluorescent probe with ultralow detection limit and high selectivity for phosgene sensing. *Dyes Pigm.* **2019**, *163*, 489−495.
(4) Wang, H.; Luo, Y.; Li, K.; Liu, B.; Gao, L.; Duan, G. Porous α-Fe_2O_3 gas sensor with instantaneous attenuated response toward triethylamine and its reaction kinetics. *Chemical Engineering Journal* **2022**, *427*, 131631.
(5) Cao, Z.; Wei, G.; Zhang, H.; Hu, D.; Yao, Q. Adsorption Property of CS_2 and COF_2 on Nitrogen-Doped Anatase TiO_2(101) Surfaces: A DFT Study. *ACS Omega* **2020**, *5*, 21662−21668.
(6) Wang, Y.; Gui, Y.; Ji, C.; Tang, C.; Zhou, Q.; Li, J.; Zhang, X. Adsorption of SF_6 decomposition components on Pt_3-TiO_2(1 0 1) surface: A DFT study. *Appl. Surf. Sci.* **2018**, *459*, 242−248.
(7) Xu, P.; Cheng, Z.; Pan, Q.; Xu, J.; Xiang, Q.; Yu, W.; Chu, Y. High aspect ratio In_2O_3 nanowires: Synthesis, mechanism and NO_2 gas-sensing properties. *Sensors and Actuators B Chemical* **2008**, *130*, 802−808.
(8) Xu, Y.; Luo, C.; Sang, H.; Lu, B.; Wu, F.; Li, X.; Zhang, L. Structure and surface insight into a temperature-sensitive CaO-based CO_2 sorbent. *Chemical Engineering Journal* **2022**, *435*, 134960.
(9) Xu, Y.; Ding, H.; Luo, C.; Zheng, Y.; Xu, Y.; Li, X.; Zhang, Z.; Shen, C.; Zhang, L. Effect of lignin, cellulose and hemicellulose on calcium looping behavior of CaO-based sorbents derived from extrusion-spherization method. *Chemical Engineering Journal* **2018**, *334*, 2520−2529.
(10) Yong, Y.; Cui, H.; Zhou, Q.; Su, X.; Kuang, Y.; Li, X. C_2N monolayer as NH_3 and NO sensors: A DFT study. *Appl. Surf. Sci.* **2019**, *487*, 488−495.
(11) Soliman, K. A.; Aal, S. A. Ti, Ni, and Cu decorated borospherene as potential molecular sensor for phosgene. *Materials Science in Semiconductor Processing* **2022**, *144*, 106574.
(12) Hussain, S.; Hussain, R.; Mehboob, M. Y.; Chatha, S. A. S.; Hussain, A. I.; Umar, A.; Khan, M. U.; Ahmed, M.; Adnan, M.; Ayub, K. Adsorption of Phosgene Gas on Pristine and Copper-Decorated $B_{12}N_{12}$ Nanocages: A Comparative DFT Study. *ACS Omega* **2020**, *5*, 7641−7650.
(13) Fiori, G.; Bonaccorso, F.; Iannaccone, G.; Palacios, T.; Neumaier, D.; Seabaugh, A.; Banerjee, S. K.; Colombo, L. Electronics based on two-dimensional materials. *Nat. Nanotechnol.* **2014**, *9*, 768−779.
(14) Zhang, R.; Lu, L.; Chang, Y.; Liu, M. Gas sensing based on metal-organic frameworks: Concepts, functions, and developments. *Journal of Hazardous Materials* **2022**, *429*, 128321.
(15) Huang, S.; Chen, K.; Li, T. Porphyrin and phthalocyanine based covalent organic frameworks for electrocatalysis. *Coord. Chem. Rev.* **2022**, *464*, 214563.
(16) De la Torre, G.; Claessens, C.; Torres, T. Phthalocyanines: Old Dyes, New Materials. Putting Color in Nanotechnology. *Chem. Commun.* **2007**, *38*, 2000−2015.
(17) Maggioni, G.; Carturan, S.; Tonezzer, M.; Quaranta, A.; Della Mea, G. Plasma-deposited copper phthalocyanine: A single gas-sensing material with multiple responses. *Sens. Actuators, B* **2008**, *131*, 496−503.
(18) Li, X.; Jiang, Y.; Xie, G.; Tai, H.; Sun, P.; Zhang, B. Copper phthalocyanine thin film transistors for hydrogen sulfide detection. *Sens. Actuators, B* **2013**, *176*, 1191−1196.
(19) Lin, L.; Li, H.; Yan, C.; Li, H.; Si, R.; Li, M.; Xiao, J.; Wang, G.; Bao, X. Synergistic Catalysis over Iron-Nitrogen Sites Anchored with Cobalt Phthalocyanine for Efficient CO_2 Electroreduction. *Adv. Mater.* **2019**, *31*, 1903470.
(20) Zou, T.; Chang, J.; Chen, Q.; Nie, Z.; Duan, L.; Guo, T.; Song, Y.; Wu, W.; Wang, H. Novel Strategy for Organic Cocrystals of n-Type and p-Type Organic Semiconductors with Advanced Optoelectronic Properties. *ACS Omega* **2020**, *5*, 12067−12072.
(21) Jogender; Badhani, B.; Mandeep; Kakkar, R. A DFT-D2 study on the adsorption of phosgene derivatives and chloromethyl chloroformate on pristine and Fe_4-decorated graphene. *Journal of Molecular Graphics and Modelling* **2020**, *101*, 107754.
(22) Zhang, T.; Sun, H.; Wang, F.; Zhang, W.; Tang, S.; Ma, J.; Gong, H.; Zhang, J. Adsorption of phosgene molecule on the transition metal-doped graphene: First principles calculations. *Appl. Surf. Sci.* **2017**, *425*, 340−350.
(23) Xia, S.; Tao, L.; Jiang, T.; Sun, H.; Li, J. Rh-doped h-BN monolayer as a high sensitivity SF_6 decomposed gases sensor: A DFT study. *Appl. Surf. Sci.* **2021**, *536*, 147965.
(24) Khan, S.; Sajid, H.; Ayub, K.; Mahmood, T. High sensitivity of graphdiyne nanoflake toward detection of phosgene, thiophosgene and phosogenoxime; a first-principles study. *Journal of Molecular Graphics and Modelling* **2020**, *100*, 107658.
(25) Sharma, A.; Khan, M. S.; Husain, M. Adsorption of phosgene on Si-embedded MoS_2 sheet and electric field-assisted desorption: insights from DFT calculations. *J. Mater. Sci.* **2019**, *54*, 11497−11508.
(26) Delley, B. From Molecules to Solids With the $DMol^3$ Approach. *J. Chem. Phys.* **2000**, *113*, 7756−7764.
(27) Perdew, J. P.; Burke, K.; Ernzerhof, M. Generalized Gradient Approximation Made Simple. *Phys. Rev. Lett.* **1996**, *77*, 3865−3868.
(28) He, C.; Wang, H.; Fu, L.; Huo, J.; Zheng, Z.; Zhao, C.; An, M. Principles for designing CO_2 adsorption catalyst: Serving thermal conductivity as the determinant for reactivity. *Chin. Chem. Lett.* **2022**, *33*, 990−994.
(29) Grimme, S. Semiempirical GGA-type density functional constructed with a long-range dispersion correction. *Journal of computational chemistry* **2006**, *27*, 1787−1799.
(30) Tkatchenko, A.; DiStasio, R. A.; Head-Gordon, M.; Scheffler, M. Dispersion-corrected Møller-Plesset second-order perturbation theory. *J. Chem. Phys.* **2009**, *131*, 094106−094112.
(31) Duan, Y.; Liu, Y.; Chen, Z.; Liu, D.; Yu, E.; Zhang, X.; Fu, H.; Fu, J.; Zhang, J.; Du, H. Amorphous molybdenum sulfide nanocatalysts simultaneously realizing efficient upgrading of residue and synergistic synthesis of 2D MoS_2 nanosheets/carbon hierarchical structures. *Green Chem.* **2020**, *22*, 44−53.
(32) Delley, B. Hardness conserving semilocal pseudopotentials. *Phys. Rev. B* **2002**, *66*, 155125.
(33) Vozzi, C.; Negro, M.; Calegari, F.; Sansone, G.; Nisoli, M.; De Silvestri, S.; Stagira, S. Generalized molecular orbital tomography. *Nat. Phys.* **2011**, *7*, 822−826.
(34) Monkhorst, H. J.; Pack, J. D. Special points for Brillouin-zone integrations. *Phys. Rev. B* **1976**, *13*, 5188−5192.
(35) Xiong, H.; Zhang, H.; Dong, J. Adhesion strength and stability of TiB_2/TiC interface in composite coatings by first principles calculation. *Comput. Mater. Sci.* **2017**, *127*, 244−250.
(36) Xiong, H.; Liu, B.; Zhang, H.; Qin, J. Theoretical insight into two-dimensional M-Pc monolayer as an excellent material for formaldehyde and phosgene sensing. *Appl. Surf. Sci.* **2021**, *543*, 148805.
(37) Cui, H.; Zhang, X.; Zhang, J.; Tang, J. Adsorption behaviour of SF_6 decomposed species onto Pd_4-decorated single-walled CNT: a DFT study. *Mol. Phys.* **2018**, *116*, 1749−1755.

https://doi.org/10.1021/acsomega.2c02548
ACS Omega 2022, 7, 21994−22002

(38) Gergen, B.; Nienhaus, H.; Weinberg, W.; McFarland, E. Chemically Induced Electronic Excitations at Metal Surfaces. *Science* **2001**, *294*, 2521−2523.
(39) Abel, M.; Clair, S.; Ourdjini, O.; Mossoyan, M.; Porte, L. Single Layer of Polymeric Fe-Phthalocyanine: An Organometallic Sheet on Metal and Thin Insulating Film. *J. Am. Chem. Soc.* **2011**, *133*, 1203−1205.
(40) Zhou, Y.; Gao, G.; Chu, W.; Wang, L. Computational screening of transition metal-doped phthalocyanine monolayers for oxygen evolution and reduction. *Nanoscale Advances* **2020**, *2*, 710−716.
(41) Wang, Y.; Yuan, H.; Li, Y.; Chen, Z. Two-dimensional iron-phthalocyanine (Fe-Pc) monolayer as a promising single-atom-catalyst for oxygen reduction reaction: a computational study. *Nanoscale* **2015**, *7*, 11633−11641.
(42) Bano, A.; Krishna, J.; Maitra, T.; Gaur, N. K. CrI_3-WTe_2: A Novel Two-Dimensional Heterostructure as Multisensor for BrF_3 and $COCl_2$ Toxic Gases. *Sci. Rep.* **2019**, *9*, 11194.
(43) Zhao, W.; Zou, D.; Sun, Z.; Yu, Y.; Yang, C. Controlling spin off state by gas molecules adsorption on metal-phthalocyanine molecular junctions and its possibility of gas sensor. *Phys. Lett. A* **2018**, *382*, 2666−2672.
(44) Zhang, J.; Ma, L.; Zhang, M.; Zhang, J. Effects of gas adsorption on electronic and optical properties of palladium-doped graphene: First-principles study. *Physica E: Low-dimensional Systems and Nanostructures* **2020**, *118*, 113879.
(45) Patel, K.; Roondhe, B.; Dabhi, S. D.; Jha, P. K. A new flatland buddy as toxic gas scavenger: A first principles study. *Journal of Hazardous Materials* **2018**, *351*, 337−345.

https://doi.org/10.1021/acsomega.2c02548
ACS Omega 2022, 7, 21994−22002